

Characteristics of Satellite Breakups from Radar Cross Section and Plane Change Angle

Gautam D. Badhwar* and Andrew E. Potter†

NASA Johnson Space Center, Houston, Texas

and

Philip D. Anz-Meador‡ and Robert C. Reynolds§

Lockheed Engineering & Sciences Company, Houston, Texas

A problem of considerable interest in orbital debris research is the determination of the cause of the fragmentation of a satellite from the observed radar cross section and orbital element data. In this paper, analytic representations of the observed distribution functions of the radar cross section and the orbital plane change angle are derived. This then allows for the extraction of a small number of features that describe the observed data. Based on the known cause of fragmentation of a subset of satellites, a linear classifier is trained on these derived features. The discriminant function derived from this training is used to determine the previously unknown cause of the satellite breakup. The technique developed is objective and has been applied to the study of the cause of a number of unknown satellite breakup events.

Introduction

THE phenomenon of on-orbit fragmentation has contributed to almost half of the current objects orbiting the earth. There are at least three major causes of these fragmentation: 1) propulsion-related explosions, 2) intentional explosions, such as antisatellite tests (ASAT), and 3) collisional or hypervelocity impacts. The resulting debris distribution depends on the mechanism of the breakup; however, current observational techniques do not allow objects of less than about 8 cm diam to be detected, even though objects as small as a few millimeters pose a potentially significant spacecraft hazard. The information about these objects has to be derived from a knowledge of the cause of fragmentation and from the fluxes of objects that can be seen, i.e., those with diameters above about 8 cm. Thus, the identification of the cause of the breakup from data on objects that can be detected is an important aspect of the orbital debris research.

Culp and McKnight¹ developed a Satellite Fragmentation Event (SAFE) Test based on the analysis of mass distribution, variations of periods and inclination, trackable mass, and asymmetry of breakup in Gabbard plots. This test assigns a score to six factors: 1) Is the mass distribution exponential? 2) Is mass distribution describable by a polynomial of small finite order? 3) What is the relative magnitude of dispersion of larger pieces of debris in the Gabbard plot? 4) How asymmetric is this dispersion? 5) the orderedness of this dispersion; and 6) the change in velocity imparted to the larger pieces. The weighting for the analytic and graphical approaches in the test scores is equal. The graphical approach is inherently subjective, and with finite errors in the observed data, a true exponential distribution can be fitted with a polynomial of only a few terms so that criteria 1 and 2 in the SAFE test may be redundant. In addition, the Gabbard plots are influenced by the age of the

debris due to atmospheric drag. Although the SAFE test is subjective, it had reasonable success when applied to 12 breakups. This suggested that a quantitative and objective approach was needed to yield more satisfactory results.

In this paper, a methodology for the characterization of the mechanism for on-orbit satellite fragmentation is developed that is objective and provides the relative probability of the satellite breakup event due to each of three major causes: 1) low-intensity explosion, 2) high-intensity explosion, and 3) hypervelocity collision. This is done by extracting simple features from the observed data to develop "signatures" that characterize each of these classes. In this paper, the distribution in fragment size (radar cross section) and orbital plane change angle were used to characterize the breakup events. A linear classifier is trained on a known set of breakup events to develop these signatures. The signatures of the unknown breakup satellites are then objectively compared to these signatures to classify the unknown events.

Approach

The approach described in this section is based on finding an analytic representation of both the radar cross section (RCS) and the orbital plane change angle distributions of the breakup event. The RCS estimates are made from the AN/FPS-85 radar operating at 442 MHz at Eglin Air Force Base, Florida, and the orbital element sets needed for the calculation of the plane change angle are provided by radars operated by the U.S. Space Command (USSPACECOM). These radars have a threshold in object size of about 8 cm diam orbiting at an altitude of 400 km. Thus, only relatively large objects from breakup events are detected. The parameters describing the frequency distribution of the radar cross section and the plane change are estimated by fitting the observed data to a derived analytic form. A statistical analysis is used to select a subset of these features that contains most of the information about the type of breakup. These parameters are then used in a supervised classification mode to classify unknown breakup events.

Section I describes the development of the models used to extract the relevant features from the radar cross section data and the plane change angle data. The model for the radar cross section is based on the experimental work of Bess.² Following this development, the analysis of these data is discussed in Sec. II and finally, in Sec. III, the features derived from this analysis are used in a supervised classification mode to classify various fragmentation events.

Received Nov. 16, 1987; revision received April 23, 1988. Copyright © 1988 American Institute of Aeronautics and Astronautics, Inc. No copyright is asserted in the United States under Title 17, U.S. Code. The U.S. Government has a royalty-free license to exercise all rights under the copyright claimed herein for Governmental purposes. All other rights are reserved by the copyright owner.

*Space Scientist.

†Supervisory Space Scientist.

‡Scientist.

§Senior Scientist.

Model Development

Radar Cross Section

Bess² experimentally examined the mass m distribution resulting from a hypervelocity impact, a high-intensity explosion, and a low-intensity explosion and showed that the cumulative mass distribution $N(>m)$ of the debris caused by a hypervelocity projectile (3.0–4.5 km/s) impact is of the form

$$N(>m) = N_o m^{-v} \quad (1)$$

where N_o and v are two constants, whereas the distribution function for explosions followed an exponential distribution in the square root of mass

$$N(>m) = N_o \exp(-c\sqrt{m}) \quad (2a)$$

m , where c is a constant. Equation (2a) can be converted to a differential frequency distribution in radar cross section R by first relating the mass m to area of the fragment A as $m = bA^\delta$ where δ , for example, varies between 0.5 for a uniform plate to 0.75 for a uniform sphere and b is related to the density. This gives

$$\frac{dN}{dA} = \frac{N_o c \sqrt{b}}{2} A \left[\frac{\delta}{2} - 1 \right] \exp \left[-c\sqrt{bA^\delta} \right] \quad (2b)$$

For the Mie scattering region, R/A is a function of the ratio $2\pi r/\lambda$, where λ is the operating wavelength of the radar and r is the radius of scattering sphere. This function is quite complicated; however, for $r < 0.1\lambda$ (Rayleigh region), it has a slope of 3 in A , and for $0.1\lambda < r < 1.6\lambda$ (Mie region), an average slope of about 1. Combining Eq. (2b) with the expression for Mie scattering suggests that the differential distribution of radar cross section R can be written as

$$\frac{dN}{dR} = KR^\alpha \exp(-\beta R^\gamma) \quad (3)$$

where α , β , and γ are constants. Note that for $\beta = 0$, this equation is a power law, and for $\alpha = 0$, an exponential law.

If the equation is normalized such that

$$\int_0^\infty \frac{dN}{dR} dR = 1$$

(note that peak RCS value is reached at the point R_m),

$$\beta = \left[\frac{\alpha}{\gamma} \right] \frac{1}{R_m^\gamma} \quad (4)$$

then the distribution function can be written as

$$\frac{dN}{dR} = \frac{\gamma[\alpha/\gamma]^{\alpha+1/\gamma}}{\Gamma\alpha+1/\gamma} \frac{1}{R_m} \left[\frac{R}{R_m} \right]^\alpha \exp \left\{ - \left[\frac{\alpha}{\gamma} \right] \left[\frac{R}{R_m} \right]^\gamma \right\} \quad (5)$$

A derivation identical to the one just followed using Eq. (1), again leads to a model of the form of Eq. (3). Thus, these three kinds of breakup events can be characterized in the RCS distribution by α , R_m , and γ . Physically, these parameters represent the asymptotic rise, the peak, and the asymptotic fall in the differential RCS distribution. It should, however, be remembered that these parameters implicitly depend on the physical density of the satellite fragments, the operating radar wavelength, the altitude, and the age of the debris fragments. A simple analysis shows that since the drag is proportional to the area, the differential distribution will shift to higher values of α , γ , and a lower value of R_m as atmospheric drag removes debris from the orbit. A more refined analysis should take these factors into account and analyze the data as close to the time of breakup as possible. Equation (5) has been used in the analysis of all the RCS data.

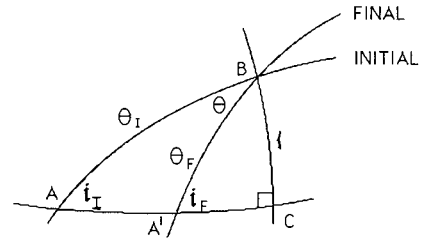


Fig. 1 The spherical triangles showing the geometry of the plane change angle calculation. The S and C are the sine and cosine of the angle, respectively.

Plane Change Angle Distribution

One of the important characteristics of a breakup process in orbit is the velocity perturbations applied to the fragments during the breakup. The velocity perturbation will, in general, change energy, angular momentum, and the plane of orbit. Of all the orbital elements that define the orbit of a given debris fragment, the inclination changes the least for the major perturbations encountered in low Earth orbit. If the inclination of the object before breakup is known, and the latitude at which it occurred is also known, the plane change angle, which essentially measures the cross-range velocity perturbation, can be determined, and this can be done using either data taken immediately after the breakup or "old" data; the quantities needed to define plane change angle do not change with time.

The spherical triangles ABC and $A'BC$ in Fig. 1 show the relationship between the plane change angle, θ , the initial and final inclination i_i and i_f , the latitude of the breakup l , and the arguments of latitude θ_i and θ_f for a breakup occurring at B , with fragments being injected from an initial orbit to a final orbit at this point. This is

$$C_\theta = \frac{C_{i_i} C_{i_f} + S_{i_i} S_{i_f} C_{\theta_i} C_{\theta_f}}{1 - S_{i_i} S_{i_f} S_{\theta_i} S_{\theta_f}} = \frac{C_{i_i} C_{i_f} + \sqrt{S_{i_i}^2 - S_1^2} \sqrt{S_{i_f}^2 - S_1^2}}{1 - S_1^2} \quad (6)$$

where $S_{\theta_i} = S_1/S_{i_i}$ and $S_{\theta_f} = S_1/S_{i_f}$. Although θ_i and θ_f cannot be determined unambiguously knowing only the latitude of the breakup, both $S_{\theta_i} S_{\theta_f}$ and $C_{\theta_i} C_{\theta_f}$ will be greater than zero in all cases except where the argument of latitude is very near 90 or 270 deg or where the velocity perturbations are extremely large.

For time-invariant calculation of the plane change angle, the latitude of the breakup event must be known. This information is taken from the work of Johnson et al.³

The insensitivity to time in the calculation of plane change angle is important because data on fragmentation events are often not available until long after the breakup occurs. However, beyond the fact that the quantities in Eq. (6) do not vary in time, the plane change angle, because it is measuring the cross-range velocity perturbation and has only a second-order effect on the energy, is less susceptible to selection effects than other characteristics, such as change in semimajor axis.

Wiesel⁴ first suggested that the plane change angle can be used to separate the type of explosion and, based on simple arguments of the equipartition of energy and a spherical explosion geometry, showed that their distribution should be Gaussian. An examination of the differential plane change angle distribution $dN/d\theta$ as a function of the plane change angle θ for number of breakups showed that the distribution is essentially Gaussian but with constant background contribution. This distribution can be parameterized by

$$\frac{dN}{d\theta} = \frac{A}{\sqrt{2\pi\sigma^2}} \exp \left[-\frac{[\theta - \theta_p]^2}{2\sigma^2} \right] + \eta \quad (7)$$

where θ_p is the peak of the distribution, σ is its variance, and η is the background level.

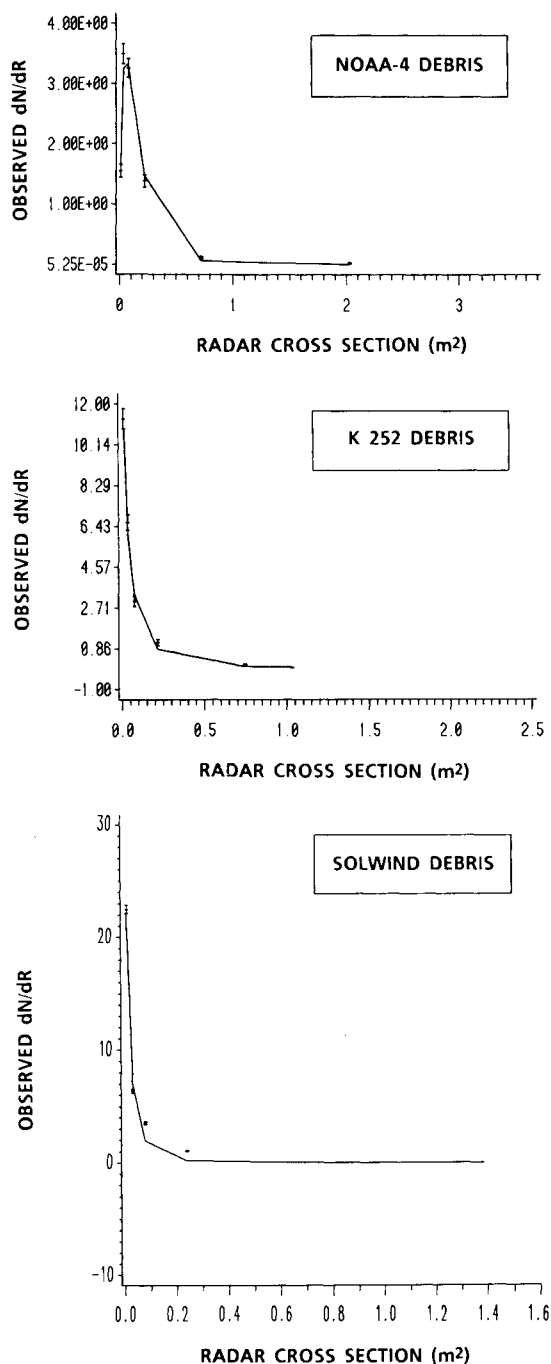


Fig. 2 A plot of the frequency distribution of the weighted radar cross section for the breakup of the NOAA-4 (low-intensity explosion), Cosmos 252 (high-intensity), and Solwind (hypervelocity). The points with error bars are the actual observed values, and the solid curve is the best fit to Eq. (5).

Analysis

Radar Cross Section

The observed RCS data were grouped into ten nonuniform intervals, and the weighted RCS values of each interval and the number of fragments falling in each interval was calculated. The grouped data were fitted to the model of Eq. (5) by a nonlinear fitting algorithm to estimate the three parameters α , R_m , and γ and their associated errors. Figure 2a shows the observed data for the NOAA-4 breakup, which was a propulsion-related low-intensity explosion breakup. The points with error bars are the data points, and the solid line is the best fit curve that joins the predicted value estimated by the best fit to Eq. (5) of the observed distribution. Figure 2b shows a similar

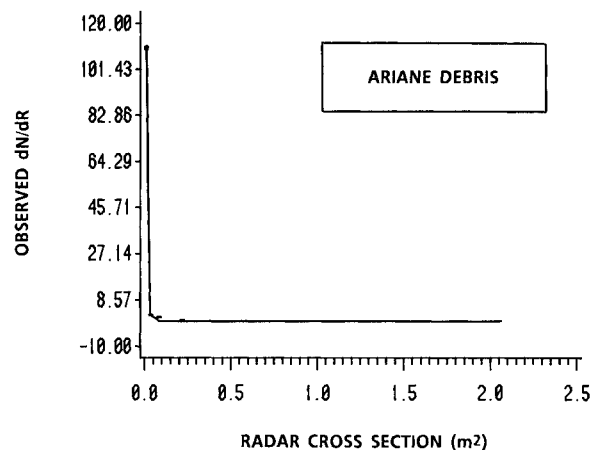


Fig. 3 A plot of the frequency distribution of the weighted radar cross section for the breakup of the Ariane second stage. Note the large number of pieces at the threshold of observation of the radar. The cause of this breakup is under investigation but currently is believed to be a high-intensity explosion.

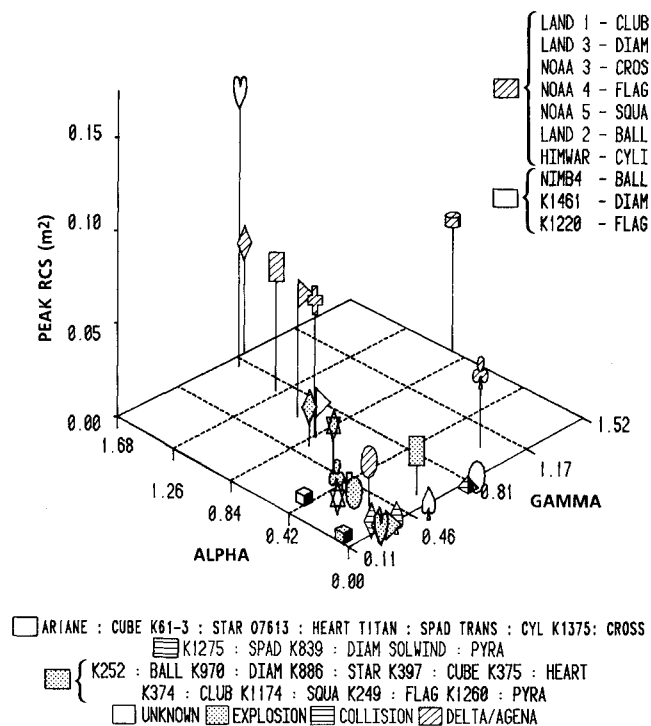


Fig. 4 A three-dimensional plot of the parameters derived from the radar cross-sectional data for the 26 breakup events. The high-intensity explosion are shown as dots, the hypervelocity impacts as horizontal stripes, the low-intensity explosion as cross stripes, and the unknown events as blank. Note that the low-intensity explosion lies above the α , γ plane and that there is a general clustering of the high-intensity explosion data.

plot for an alleged Soviet ASAT test Cosmos 252 destroyed by a high-intensity explosion.³ The Cosmos 252 curve is quite steep compared to the NOAA-4 breakup. Figure 2c is a plot of the only definitely known hypervelocity impact breakup event (Solwind). The frequency distribution is more like that of the Cosmos 252 breakup and less like that of the NOAA-4 breakup. Figure 3 is the same plot of the 226 fragments resulting from the breakup (cause unknown, although the explosion story is most likely) of the Ariane second stage. It shows that the distribution may be even steeper than the Cosmos 252 breakup. As was expected from the earlier discussion, the RCS distribution can indeed be described by the model of Eq. (5).

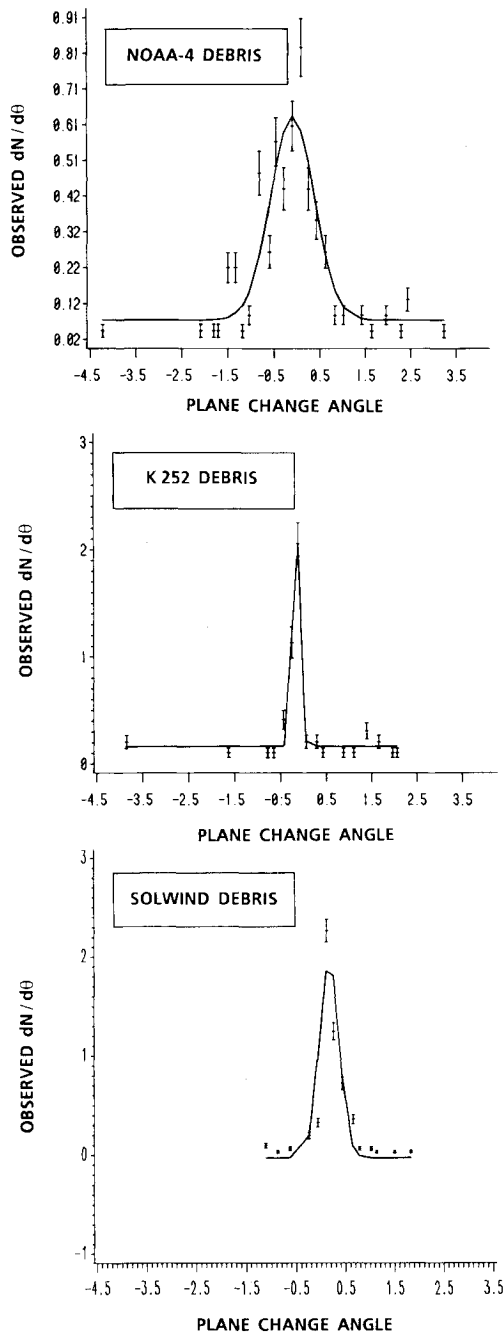


Fig. 5 A plot of the frequency distribution of the plane change angle for the breakup of the NOAA-4 (low-intensity), Cosmos 252 (high-intensity), and Solwind (hypervelocity impact). The points with error bars are the observed values, and the solid curve is the best fit to the Gaussian equation, Eq. (7).

Figure 4 is a plot of the α , R_m , and γ for all of the breakup events for which RCS data are available. The symbols identify the various parent satellites and the shades identify the currently believed cause of the breakup. Much of this information is derived from Johnson et al.³ It is, however, clear that all the low-intensity explosions lie substantially above the α , γ plane. It also should be pointed out that the values of γ and α observed are in rough qualitative agreement with values for explosions as seen in the work of Bess.² They are also in accord with Bess's observation that c for a high-intensity explosion is greater than for a low-intensity explosion. This figure suggests a rough classification scheme: collision-type breakups are defined by $R_m \sim 0$, high-intensity explosions by $R_m \sim 0$, $\alpha > \gamma$, and low-intensity explosions by $R_m > 0.05$ and $\alpha, \gamma > 0.3$.

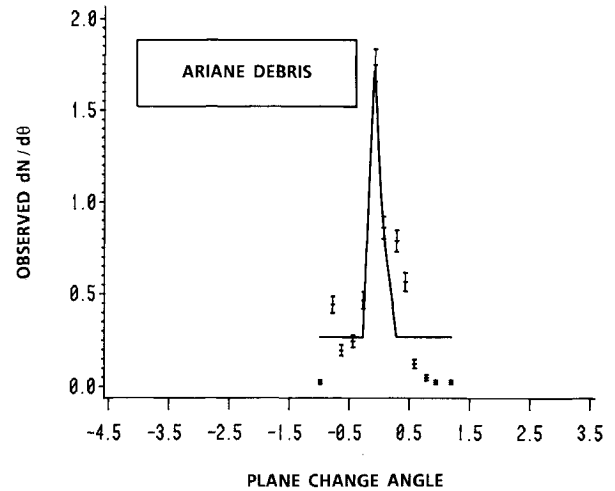


Fig. 6 A plot of the frequency distribution of the plane change angle for the breakup of the Ariane second stage. The fit to data is not as good as in the case of the NOAA-4 and Cosmos 252 breakups. However, the central peak is very narrow. This suggests that this breakup is a high-intensity explosion.

The technique described differs substantially from the work of Culp and McKnight¹ in that they work with the cumulative mass density distribution and thus require a knowledge of the spacecraft density, or more precisely, the fragment densities, and that they do not consider the effects of Mie scattering on the relation between size and RCS. They also do not have a single model to describe all types of breakup events.

It has been shown that the RCS data can be fitted to a single three-parameter model that has experimental support and that these parameters permit a rough separation of breakup types. In the next section, information deduced from the plane change angle data is described.

Plane Change Angle Analysis

The plane angle data for each breakup event were grouped into 0.18-deg intervals, and the differential number density $dN/d\theta$ was computed such that the total area under the curve is unity. This normalized distribution was fitted to the model of Eq. (7) and the parameters corresponding to the peak of the distribution, its variance, and the background values estimated. The accuracy with which the plane change angle can be computed depends on the precise knowledge of the breakup latitude and longitude, which, if accurately known, give better than 0.1-deg accuracy in plane change. As already mentioned, the plane change angle is relatively insensitive to the age of the breakup. Figure 5a shows the plane change angle θ distribution for the NOAA-4 fragmentation. The error bars again correspond to the number of fragments in each interval, and the fluctuations are caused by a very fine interval size. The solid curve is the best fit to the data using Eq. (6). Figures 5b and 5c show similar plot for Cosmos 252, an alleged ASAT high-intensity explosion, and Solwind, the only definitely known hypervelocity impact breakup event. The Cosmos 252 and Solwind breakups have narrow distributions compared to the NOAA-4 distribution. This is what one might expect because a low-intensity explosion would, like an overpressurized balloon, more likely scatter the debris into a large angular range than would a high-intensity explosion. Figure 6 shows the same plot for the debris from the Ariane V16 breakup. However, because of the smaller range of data, the interval is 0.05 deg. This distribution is extremely narrow and much more like a high-intensity explosion than a low-intensity explosion. There are two asymmetric secondary peaks on either side of the central peak. The variance of these peaks is quite comparable to that of the central peak. An examination of the RCS data of these secondary peaks shows no particular difference from the RCS distribution of the main peak. The reasons for these peaks are

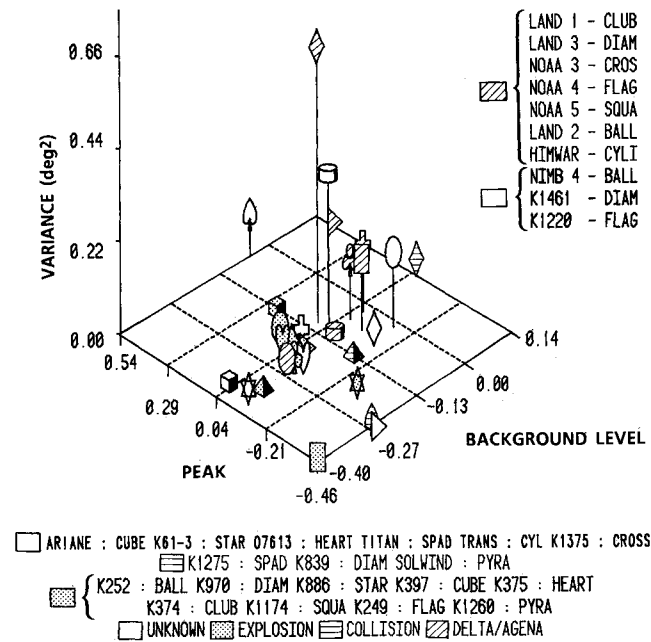


Fig. 7 A three-dimensional plot of the parameters derived from fitting the plane change angle frequency distribution for the breakup events. Note that the location of the peak of the plane change angle distribution provides no separation into classes and that much of the separation information is contained in the measure of the variance.

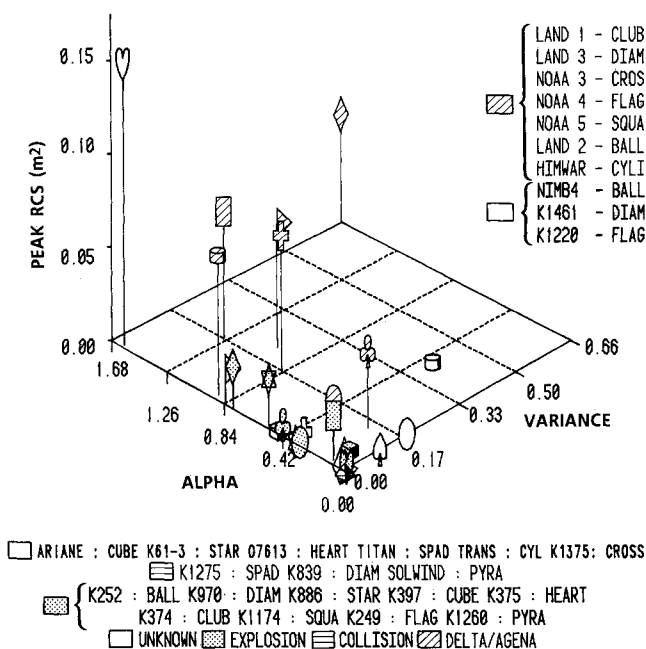


Fig. 8 A three-dimensional plot of the parameters σ , α , and γ for breakups. From Figs. 4 and 7 it is clear that information from the radar cross section or the plane change angle by itself is not sufficient for class separation but that combining the two gives a better measure of separation.

not understood but may well be the accuracy with which θ can be calculated. In subsequent analysis, the variance of the central peak distribution is used.

Figure 7 is the plot of the variance, the peak, and the background level of the plane change angle distribution for all of the breakup events. The high-intensity explosions are all clustered around low variance values and the low-intensity explosion around high variance values. The exception is the Landsat 2 upper stage breakup. This event was characterized by two breakup events and should have been treated as such. As expected, the peak values do not allow any separation because it

tells more about which way the momentum transfer took place and not why the breakup occurred. The background values do provide some separation; however, the error in its determination is typically large because of the poor statistics at the tail ends of the distribution.

Analysis of the Combined Radar Cross Section and Plane Change Angle Data

A principal component analysis of all of the derived features shows that the features α , R_m , and σ carry most of the information on the class of the breakup event. It should be emphasized that other features derived from the angular momentum transfer, energy, or velocity perturbations may be more powerful discriminators of breakup type but have not been carefully analyzed.

From Figs. 4 and 7 it can be seen that neither the RCS-derived parameters nor the plane change angle-derived parameters individually are sufficient to separate the type of breakup. Furthermore, only the variance of the plane change angle is important among the plane change-derived parameters. However, combining the two sets of parameters does lead to a better separation. This is shown in Fig. 8, a plot of the σ , α , and R_m , which shows that the separation into three classes is indeed better than that indicated in either Fig. 4 or 7. The next section describes the method of classification using the four features previously discussed.

Classification of Breakup Events

For the set of breakup events containing the variables α , R_m , γ , and σ and a classification variable defining the group of breakup (high-intensity explosion, low-intensity explosion, and hypervelocity impact), a linear discriminant function or classification criterion can be determined. This is defined by a measure of the generalized squared distance⁵

$$D_t^2(x) = g_t(x, t) + g(t) \quad (8)$$

where x is the vector of observations and t a subscript to distinguish the group,

$$g_t(x, t) = (\bar{x} - \bar{\mu}) \sum_t^{-1} (x - \mu) + 1n \left| \sum_t \right| \quad (9)$$

and $g(t) = 0$ if all classes are equally probable and $= -1n$ (the prior probability for group t). The vector μ contains the means of the variable in the group t , and Σ is the covariance matrix.

The posterior probability of an observation x belonging to the group t is

$$p_t(x) = \frac{\exp[-0.5D_t^2(x)]}{\sum_t \exp[-0.5D_t^2(x)]} \quad (10)$$

An observation belongs to the group $t=k$ if $D_k^2(x)$ is the least or $p(x)$ is the highest value.

Table 1 Classification of debris known data

Type	Number of observations and percentages classified into type			
	C	D	E	Total
C	3 100.00	0 0.00	0 0.00	3 100.00
D	0 0.00	7 100.00	0 0.00	7 100.00
E	1 14.29	0 0.00	6 86.71	7 100.00
Total	4	7	6	17
percent	23.53	41.18	35.29	100.00

Table 2 Classification of debris known data

Posterior probability of membership in type:					
Satellite	Type	Classified into type	C	D	E
Cosmos 839	C	C	0.6031	0.0000	0.3969
Solwind	C	C	0.9185	0.0000	0.0815
Cosmos 1375	C	C	0.6988	0.0000	0.3012
Hiwari	D	D	0.0000	1.0000	0.0000
Landsat 1	D	D	0.0000	1.0000	0.0000
Landsat 3	D	D	0.0000	1.0000	0.0000
NOAA 3	D	D	0.0000	1.0000	0.0000
NOAA 4	D	D	0.0000	1.0000	0.0000
NOAA 5	D	D	0.0000	1.0000	0.0000
Landsat 2	D	D	0.0605	0.9034	0.0361
Cosmos 252	E	E	0.3228	0.0000	0.9772
Cosmos 970	E	E	0.0826	0.0000	0.9174
Cosmos 886	E	E	0.2141	0.0000	0.7858
Cosmos 397	E	E	0.4724	0.0000	0.5276
Cosmos 375	E	C ^a	0.6205	0.0000	0.3795
Cosmos 374	E	E	0.2166	0.0000	0.7834
Cosmos 1174	E	E	0.0377	0.0000	0.9623

^aMisclassified observation (probably due to mixing of K 374 and K 375 orbital elements). C = hypervelocity impact, D = low-intensity explosion, E = high-intensity explosion.

The discrimination procedure was trained on breakup events of known category, and then the same observations were reclassified. This gives the best possible performance of the classifier. It should be noted that the accuracy of any such classifier depends on how well the training class samples the actual class distribution, and since there are only three known or suspected hypervelocity impact events, this increases the uncertainty with which this class can be identified.

The division of all the breakup events into these three classes is based on the work of Bess;² however, it is quite arbitrary in the sense that each explosion is unique in its energetics and the location of the detonation charge on the body. Similarly, the collision can be head-on or glancing. Thus, in each class there exists a distribution of parameters that describes that overall class. This is only a first-order broad classification.

Table 1 gives the confusion matrix, and Table 2 gives the actual breakdown of the posterior membership probabilities. Cosmos 375 is misclassified. It is believed that the orbital elements of the fragments from the breakup of Cosmos 374 and 375 have been mixed.⁶ Using the training statistics developed, the breakup events labeled black (hollow) were classified.

A comparison of these results with the work of Culp and McKnight (1986) shows good agreement in two-class separation, i.e., low-intensity explosion (called propulsion related by Culp and McKnight) and high intensity + hypervelocity breakups. Nimbus 4, although thought to be a propulsion-related breakup, is not classified as propulsion-related in this study or in Culp and McKnight's analysis. However, Cosmos 1275 is considered to be a hypervelocity impact by Culp and McKnight, whereas this analysis shows only a 38.1% probability for impact. OPS 7613 is a Delta class breakup and is so classified. In this analysis, Cosmos 1461 is misclassified as a collision whereas it is considered to be a high-intensity explosion.³ In this case, there were two distinct breakup events that occurred at different times. They have been treated as one in this analysis. A more refined analysis would treat them as separate events, hence, the misclassification.

The analysis of the Ariane V16 breakup shows that it was a high-intensity explosion with a probability of 89.6% and a collision with a probability of 10.4%. If one assumes that Cosmos 1275 is a collisional breakup and reclassifies the data accordingly, Ariane would show probabilities of 78.6 and 21.4%, respectively, for the same two categories. It was mentioned earlier that there are secondary peaks on either side of the central peak in the plane change angle differential distribution and that the variance of the central peak was used in the anal-

Table 3 Classification of debris unknown data, posterior probability of membership in type

Satellite	Type	Classified into type	C	D	E
Ariane	U	E	0.2142	0.0000	0.7858
Cosmos 1275	U	E	0.3813	0.0000	0.6187
Cosmos 61-63	U	F	0.3147	0.0000	0.6853
Nimbus 4	U	C	0.9328	0.0000	0.0672
OPS7613	U	D	0.0000	1.0000	0.0000
Titan 3C	U	C	0.8198	0.0000	0.1802
Transit	U	C	0.8816	0.0005	0.1178
Cosmos 1461	U	C	0.5510	0.0000	0.4490
Cosmos 1220	U	E	0.1358	0.0000	0.8642

ysis. The given results are not affected if the data is binned in coarser bins and refitted to smooth out the secondary peaks. This is because this distribution is extremely narrow to begin with.

This conclusion differs from the analysis of Benz et al.⁷ who concluded that the breakup of Ariane's third stage was caused by a physical pressure burst, i.e., the pressure source is of nonchemical means, such as inert gas pressure. This analysis was based on a comparison of the predicted fragment velocities based on models of exploding orbital tanks to the fragment velocities calculated from the observed orbital elements of the fragments, an analysis of the debris pattern, and a comparison of the total energy calculated for the debris with total energy calculated for the explosion based on theoretical models. Their calculation assumed that the radar observed most of the debris, and the orbital parameters are known with great precision. Both of these assumptions are not quite correct. Indeed, about two-thirds of the fragments are not seen by the radar. Benz et al.⁷ do suggest that the initial failure of the tanks could have been caused by a collision of small particles or a linear-shaped destruct charge, or from fatigue of the tanks or failure of the bulkhead that separates the fuel tanks. Our results can be consistent with the analysis of Benz et al.⁷ if the physical pressure burst mechanism advocated by them produces an extremely narrow plane change angle distribution. If so, the definition of high-intensity explosions suggested by Bess² needs to be enlarged to encompass such events.

Neumann⁸ stated that Ariane engineers had concluded that a possible cause of the breakup was leakage from the hydrogen tank. When pressure in the hydrogen tank dropped below that

in the oxygen tank, the bulkhead separating the two chambers reversed, broke, and initiated a catastrophic breakup of the entire structure.

Conclusions

1) A three-parameter model that describes the differential RCS distribution has been developed. This model is related to laboratory-derived mass distributions for various breakup categories and permits a classification for various satellite breakups. However, these parameters depend on age and fragment density.

2) A parametric representation of the plane change angle differential distribution has been found. It is shown that the variance of this distribution is an effective separator of breakup classes.

3) A linear discriminant procedure trained on known breakup events has been used to classify unknown breakups. The results are in general agreement with the work of Culp and McKnight,¹ although they do differ in specific cases.

4) Additional information derived from the orbital elements such as angular momentum, energy change, decay rates, and so forth, should be examined to further refine the classification results. The age dependence of the RCS data distribution

should also be taken into account.

5) A clear need to identify additional hypervelocity impact events exists. The signatures of these events are very firmly established.

References

- ¹Culp, R. D. and McKnight, D. S., "Analysis of the Origins of Debris Clouds," Teledyne Brown Engineering, Colorado Springs, CO, CR SC 7460, Oct. 1986.
- ²Bess, T. D., "Mass Distribution of Orbiting Man-Made Space Debris," NASA Langley Research Center, Hampton, VA, Rept. L-10477, Dec. 1975.
- ³Johnson, N. L., Gabbard, J. R., Kling, R. L., Jr., and Jones, T. W., "History of On-Orbit Satellite Fragmentation," Teledyne Brown Engineering TR CS 86-USASDC-001, Feb. 1986.
- ⁴Wiesel, W., "Fragmentation of Asteroids and Artificial Satellites in Orbit," *ICARUS*, Vol. 34, April 1978, pp. 99-116.
- ⁵Rao, C. R., "Linear Statistical Inference and its Applications," Wiley, New York, 1973.
- ⁶Johnson, private communication, May 1987.
- ⁷Benz, F. J., Bishop, R. L., and Eck, M. B., "Explosive Fragmentation of Orbiting Propellant Tanks," Upper Stage Break Up Conference, Johnson Space Center, Houston, TX, May 1987.
- ⁸Neumann, J., private communication, July 1987.

Recommended Reading from the AIAA Progress in Astronautics and Aeronautics Series . . .



Opportunities for Academic Research in a Low-Gravity Environment

George A. Hazelrigg and Joseph M. Reynolds, editors

The space environment provides unique characteristics for the conduct of scientific and engineering research. This text covers research in low-gravity environments and in vacuum down to 10^{-15} Torr; high resolution measurements of critical phenomena such as the lambda transition in helium; tests for the equivalence principle between gravitational and inertial mass; techniques for growing crystals in space—melt, float-zone, solution, and vapor growth—such as electro-optical and biological (protein) crystals; metals and alloys in low gravity; levitation methods and containerless processing in low gravity, including flame propagation and extinction, radiative ignition, and heterogeneous processing in auto-ignition; and the disciplines of fluid dynamics, over a wide range of topics—transport phenomena, large-scale fluid dynamic modeling, and surface-tension phenomena. Addressed mainly to research engineers and applied scientists, the book advances new ideas for scientific research, and it reviews facilities and current tests.

TO ORDER: Write AIAA Order Department,
370 L'Enfant Promenade, S.W., Washington, DC 20024
Please include postage and handling fee of \$4.50 with all
orders. California and D.C. residents must add 6% sales
tax. All foreign orders must be prepaid.

1986 340 pp., illus. Hardback
ISBN 0-930403-18-5
AIAA Members \$59.95
Nonmembers \$84.95
Order Number V-108